

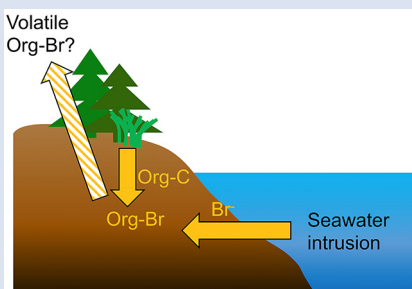
Sea level rise produces abundant organobromines in salt-affected coastal wetlands

C. Joe-Wong^{1,†*}, D.R. Schlesinger^{2*}, A.T. Chow³, S.C.B. Myneni²



doi: 10.7185/geochemlet.1911

Abstract



Global sea level rise exposes terrestrially derived natural organic matter to elevated salinities, which may alter the complex biogeochemical cycling of halogens in coastal wetland sediments. Here we show that sea level rise increases the natural production of organobromines in submerged soils and wetland sediments. We compared the concentrations and speciation of sedimentary chlorine and bromine along a salinity gradient in low-lying coastal forested wetlands in Winyah Bay (South Carolina, United States). Sorption differences between chloride and bromide were not observed, but up to 80 % of total retained bromine is organically bound, with the highest fraction of organically bound bromine found in formerly freshwater wetlands inundated by seawater. Wet/dry cycling of soils and the abundance of aromatic-rich natural organic matter in these salt-affected

dieback forested wetlands promote bromination of organic matter, as demonstrated by laboratory simulations. Bromination of soil organic matter caused by continued sea level rise thus may be a major source of organobromines in coastal environments and possibly volatile halomethanes.

Received 18 January 2019 | Accepted 26 March 2019 | Published 23 April 2019

Introduction

Global warming and associated rises in sea level threaten to alter the biogeochemistry of coastal ecosystems. Flooding of coastal freshwater wetlands exposes their vegetation and soil-bound natural organic matter (NOM) to seawater and ultimately results in conversion to salt marshes (Doyle *et al.*, 2007; Hilton *et al.*, 2008; Krauss *et al.*, 2009). The increased salinity alters the abundance and composition of NOM in salt-affected wetlands (Goñi and Thomas, 2000; Neubauer, 2013), due to changes in vegetal inputs (Tuxen *et al.*, 2011) and microbial activity (Morrissey *et al.*, 2014). Conversely, reactions with previously inaccessible terrestrially derived NOM may also alter the biogeochemical cycling of halogens.

Both chlorine (Cl) and bromine (Br) undergo complex biogeochemical cycling in marine and soil systems. During NOM decomposition, inorganic Cl⁻ and Br⁻ react with NOM both abiotically and biotically to form halogenated organic compounds (organochlorines and organobromines, respectively) (Leri and Myneni, 2010, 2012). Understanding the natural formation of organohalogens is important in order to evaluate the stability of these compounds and their potential breakdown and release as volatile halomethanes. Many halomethanes are known to catalytically destroy stratospheric

ozone (Molina and Rowland, 1974), and coastal ecosystems such as salt marshes contribute as much as 10 % of halomethane emissions in the atmosphere (Rhew *et al.*, 2000). It is thus crucial to determine how global sea level rise may affect the biogeochemistry of halogen cycling in coastal ecosystems.

In this study, we evaluate the impacts of seawater intrusion on the production of organohalogens in wetland sediments as a first step towards predicting future halomethane emissions. The study site is located on the southeastern coast of the United States (Winyah Bay, South Carolina, United States) (Fig. S-1) (Titus and Richman, 2001). Winyah Bay is a tidally influenced forest-marsh, backwater-dominated, low-lying wetland ecosystem that has experienced severe saltwater intrusion, successively converting forested freshwater wetland to a salt-affected wetland and salt marsh over a short distance (~5 km) (Krauss *et al.*, 2009). The freshwater and salt-affected wetlands experience seasonal wet and dry cycles based on precipitation. In contrast, the salt marsh is always saturated, although water depth varies with daily tidal cycles. Vegetation varies significantly with salinity (Krauss *et al.*, 2009; Chow *et al.*, 2013). To assess the importance of NOM origin and composition, we compared the effects of increased salinity on freshwater wetland soils from Winyah Bay and on temperate forest soils from pine lands in New Jersey.

1. Department of Chemistry, Princeton University, Princeton, NJ 08544, USA

2. Department of Geosciences, Princeton University, Princeton, NJ 08544, USA

3. Biogeochemistry and Environmental Quality Research Group, Clemson University, Georgetown, SC 29440, USA

† Current address: Department of Geological Sciences, Stanford University, Stanford, CA 94305, USA

* Corresponding author (email: joe Wong@stanford.edu; drs3@princeton.edu)



Methods

Methodological details are available in the Supplementary Information. In brief, three sites at Winyah Bay spanning a range of salinities were sampled along a transect from the freshwater wetland to the salt-affected wetland and the salt marsh (Fig. S-1). 18–24 cm soil cores were collected between July 2012 and December 2016. At least two cores were taken at each site to assess variability. Additionally, a 30 cm soil core was collected from the Pine Barrens in New Jersey to determine whether halogenation reactions occur in other ecosystems.

The functional group composition of organic carbon was assessed using Fourier transform infrared (FTIR) spectroscopy and solid state ^{13}C nuclear magnetic resonance (NMR) spectroscopy. Cl and Br concentrations and speciation were determined using X-ray fluorescence (XRF) and synchrotron-based 1s X-ray absorption near edge structure (XANES) spectroscopy respectively.

Results and Discussion

Both the concentrations and the speciation of sediment-bound Cl and Br vary between the different sites, as expected. The average concentration of Cl (Cl_{total}) increases linearly with salinity: from $0.14 (\pm 0.07) \text{ g.kg}^{-1}$ in freshwater wetland sediments to $6 (\pm 1)$ and $27 (\pm 2) \text{ g.kg}^{-1}$ in the salt-affected wetland and salt marsh, respectively (Table S-1). The variability shown in the parentheses arises from differences between the two sampled cores, which were minimal, and between different depths and seasons. Cl concentrations decrease with depth in the freshwater and salt-affected wetlands, consistent with soil studies where Cl concentrations are reported to decrease sharply below the top organic-rich horizons (Leri and Myneni, 2010; Krzmarzick *et al.*, 2012). The absence of such a trend with depth in the salt marsh may be caused by homogenisation *via* tidal action. The speciation of Cl also varies with salinity, as shown by Cl XANES spectroscopy (Fig. 1). Most Cl in the top layers of freshwater sediments is organically bound (Cl_{org}), although Cl speciation in the lower layers ($> \sim 14 \text{ cm}$) could not be determined due to the low concentration of Cl. In contrast, salt-affected wetland and salt marsh samples at all depths show predominantly inorganic Cl^- (Fig. 1). The presence of Cl_{org} cannot be ruled out in the latter samples but is expected to be less than 6 % of Cl_{total} (Leri *et al.*, 2006). Variability in Cl speciation between the two cores collected at each site was also minimal.

The abundance and speciation of Br significantly differ from the behaviour of Cl. Total Br concentrations (Br_{total}) averaged over depth and between two separately collected cores increase from $13 (\pm 10) \text{ mg.kg}^{-1}$ in the freshwater wetland to $120 (\pm 50)$ in the salt-affected wetland but increase only marginally to $160 (\pm 14) \text{ mg.kg}^{-1}$ in the salt marsh despite the roughly threefold increase in water salinity. Similar to Cl, most Br in the freshwater sediments is in the form of organically bound Br (Br_{org}) (Fig. 2, Table S-1), although variations between wet and dry seasons are observed (Fig. S-3), which may be due to both temporal and spatial heterogeneity. More than 80 % of Br in the salt-affected wetland and 50 % of Br in the salt marsh is present as Br_{org} , in contrast to the predominance of inorganic Cl^- at these two sites.

The large difference in Br:Cl ratios for seawater and sediments is striking. Br:Cl ratios in all sediments are greater than the Br:Cl ratio in seawater by a factor ranging from a maximum of 26.5 in the freshwater wetland to a minimum of 1.5 in the salt marsh. Cl^- and Br^- ions are considered inert and

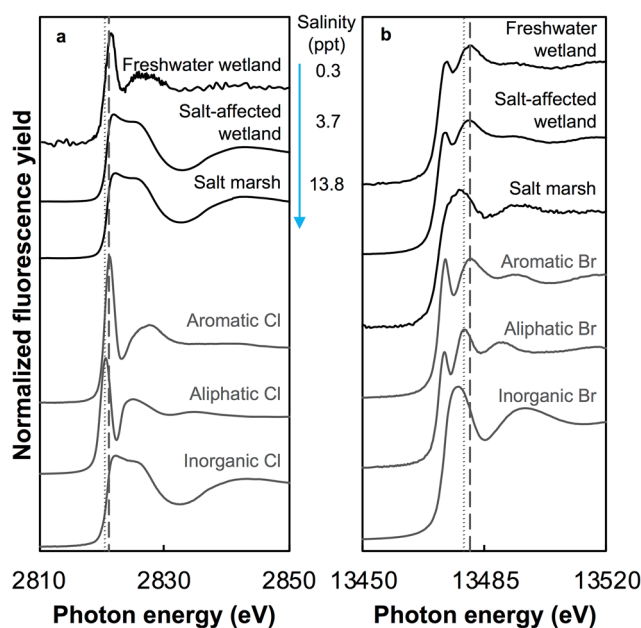


Figure 1 (a) Cl and (b) Br XANES spectra of top layer of sediments ($\sim 0\text{--}4 \text{ cm}$) on top (black) and standards (grey) at the bottom. Cl standards are chlorophenol red, chlorodecane, and NaCl (aq) for aromatic, aliphatic, and inorganic Cl respectively. Br standards are bromophenol blue, 1-bromoicosane, and KBr for aromatic, aliphatic, and inorganic Br respectively. Grey dotted and dashed lines show the spectral maxima for aliphatic and aromatic organohalogen standards respectively.

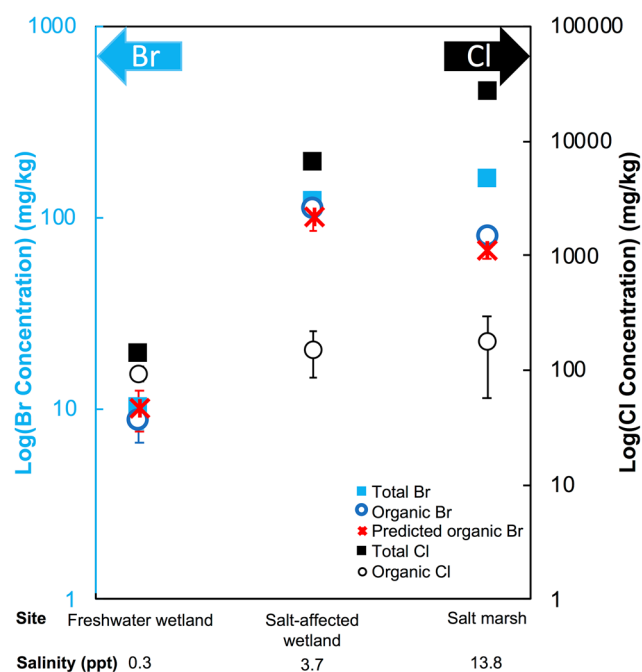


Figure 2 The concentration and speciation of Br (left, blue y axis) and Cl (right, black y axis) in sediments as a function of salinity (x axis) in Winyah Bay, South Carolina. All concentrations are the average of samples from different depths and two cores. Vertical error bars show the standard error and are in some cases smaller than the points.

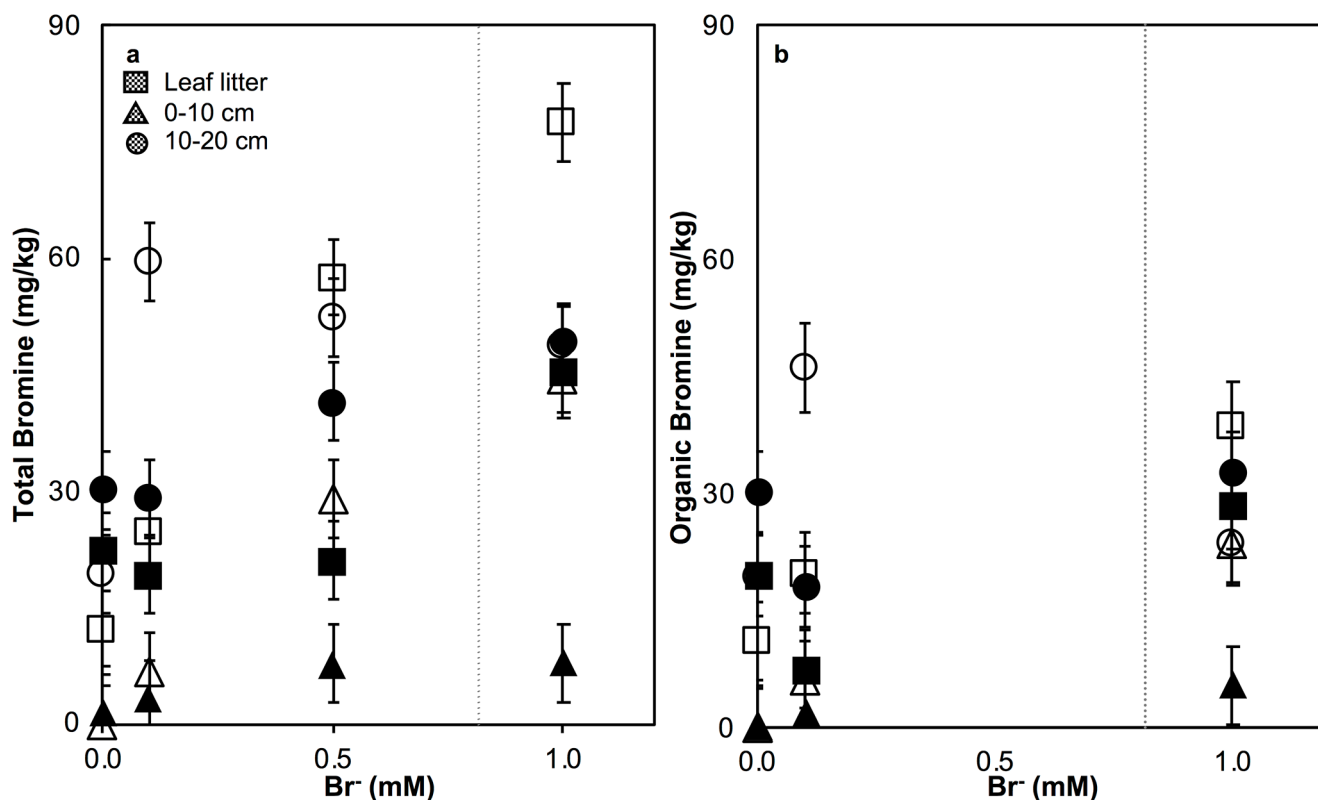


Figure 3 (a) Total Br and (b) organically bound Br produced in Br⁻-reacted soil samples as a function of increasing aqueous Br⁻ concentrations. Filled shapes (●) represent saturated conditions (mimicking salt marsh conditions) and open shapes (○) represent wet/dry conditions (mimicking salt-affected wetland conditions). Vertical gray dotted line shows Br⁻ concentration in seawater in both panels. Error bars are based on replicate XRF analyses (total Br and organic Br) and error from XANES linear combination fitting for organic Br.

exhibit similar weak sorption onto sediments, so the disproportionate retention of Br compared to Cl cannot be explained by differences in partition coefficients between sediment and water ($K_d(\text{Cl}^-) \approx K_d(\text{Br}^-)$). The measured $K_d(\text{Cl}^-)$ is small and varies between 0.2 and 1.8 with the lowest values in the freshwater wetland (Table S-1). These differences in K_d values are likely caused by differences in sediment characteristics (e.g., mineralogy, particle size, organic matter content) and depth averaged salinity values. However, the amounts of sorbed Br⁻ predicted using $K_d(\text{Cl}^-)$ are much smaller than the observed levels of Br_{total}. The excess Br is likely retained in the sediment as Br_{org}, and the abundance of Br_{org} determined spectroscopically matches well with this calculated excess (measured Br_{total} – calculated sorbed Br⁻) (Figs. 2 and S-4).

The concentration and speciation of sediment-bound Cl and Br differ significantly along the salinity gradient due to the geochemical differences between the halides and between these sites. In general, bromination of organic matter greatly exceeds chlorination. At all sites and all depths, the fraction of organically bound Br ($\text{Br}_{\text{org}}/\text{Br}_{\text{total}}$) is greater than the fraction of organically bound Cl ($\text{Cl}_{\text{org}}/\text{Cl}_{\text{total}}$) (Table S-1). This is likely because Br⁻ is both more polarisable and less electronegative than Cl⁻, aiding organic molecule halogenation reactions, which are commonly electrophilic addition reactions (Butler and Walker, 1993; Leri and Myneni, 2012).

In addition, the high abundance of NOM (Table S-2) and its high aromaticity (Figs. S-5-S-7) likely support preferential bromination of NOM in the salt-affected wetland, even though the salinity at that site is much less than in the salt marsh. In the salt-affected wetland, salt water intrusion and increases in halide concentrations stress the freshwater plants, such as bald cypresses, and reduce their productivity, ultimately leading to forest dieback and conversion to salt marsh (Munns and

Tester, 2008; Chow *et al.*, 2013; Neubauer, 2013). This adds a large amount of fresh plant biomass and NOM to the sediment (Table S-2), and ¹³C NMR and FTIR spectroscopies of this NOM shows that it is rich in aromatic carbon when compared to other sites (Figs. S-5-S-7). Aromatic organic carbon is known to promote electrophilic addition of halides (Myneni, 2002; Leri and Myneni, 2012). The salt-affected wetlands also experience wet/dry conditions with seasons and thus promote extensive redox cycling of reactive Fe and Mn oxides, which are known in turn to promote halogenation reactions (Comba *et al.*, 2015; Leri and Ravel, 2015; Lin *et al.*, 2016). The loss of plant cover in these salt-affected wetlands may also promote photolytic reactions. In contrast to salt-affected wetlands, Br_{org} production is limited in freshwater wetlands by access to Br⁻ and in salt marshes by the low abundance of reactive NOM and permanent water-saturated conditions.

Laboratory experiments conducted on freshwater wetland sediments to simulate geochemical conditions in salt-affected wetlands (wet/dry cycles, relatively low salinity) and salt marshes (saturated conditions, relatively high salinity) reproduced the field observations and trends (Fig. 3). Br_{total} retained by sediments increased with exposure to elevated Br⁻ concentration in all samples rapidly (within hours). However, the samples exposed to wet/dry conditions, mimicking salt-affected wetland conditions, in general retained more Br_{total} and produced more Br_{org} than the samples exposed to saturated conditions, mimicking salt marsh conditions (Fig. 3). No consistent trend with depth is apparent, and elevated levels of Cl⁻ and sample pH did not influence Br_{org} production significantly (Fig. S-8). Reactions of New Jersey soils with organic matter with Br⁻ also produced extensive Br_{org} (Fig S-9). Organic matter in the New Jersey soils is derived from pine, maple, and oak, so its functional group composition is expected to differ from the Winyah Bay sediments, whose organic matter

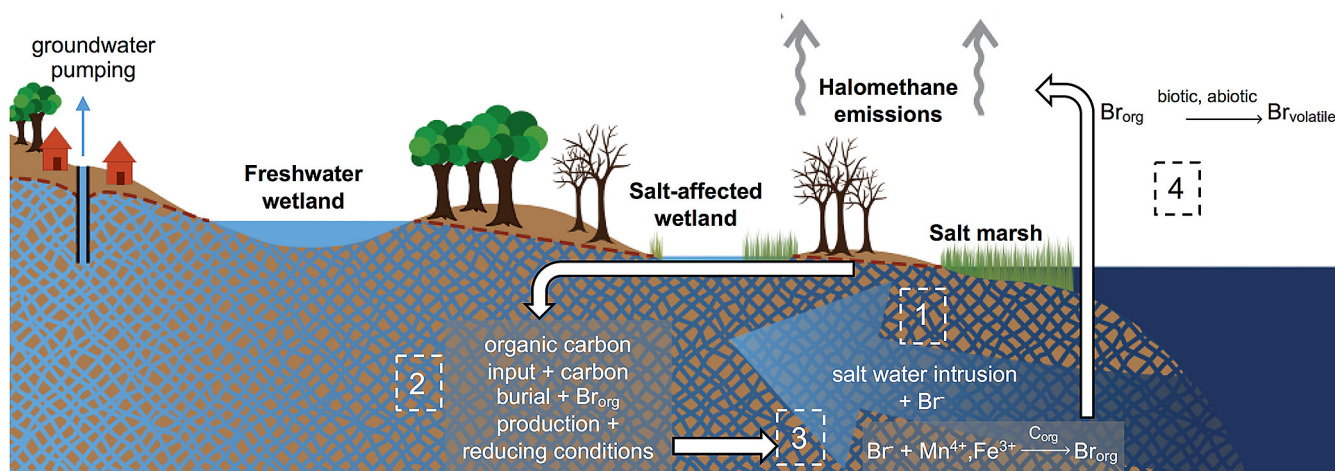


Figure 4 Schematic diagram showing organic carbon bromination and release of volatile organobromines occurring during coastal flooding by seawater. The reactions begin with seawater intrusion (1), followed by highly favourable Br_{org} production aided by geochemical conditions (2, 3), and ultimately the breakdown and release of this Br_{org} as volatile compounds into the atmosphere (4).

primarily derives from bald cypress, water tupelo, and swamp tupelo (Chow *et al.*, 2013). In contrast to the Winyah Bay freshwater wetland sediments, the production of Br_{org} in the New Jersey soil is greater in the soil O-horizon, where the reactive NOM is more abundant, than in mineral-rich lower horizons. These results suggest that the extensive bromination observed in the Winyah Bay salt-affected wetland sediments is not unique to this site but rather may occur in many types of soils and sediments with varying sources of organic matter if they are affected by saltwater intrusion.

Both field and laboratory studies indicate that sedimentary NOM can be brominated when exposed to seawater. Bromination of NOM is consistently favoured over chlorination, resulting in the accumulation of organobromines in sediments. Intrusion of salt water in coastal regions caused by sea level rise and extensive pumping of groundwater exposes freshwater sediments and surface and subsurface soils to elevated salt levels (Fig. 4). This introduces Br^- to aromatic-rich terrestrial NOM, and Br_{org} production is likely to increase in all these environments (Fig. 4). The lability of this Br_{org} is unclear. Increased flooding of salt-affected wetlands by seawater increases sulphate concentrations, which stimulates microbial sulphate reduction and accelerates organic carbon decomposition and the microbially mediated reductive debromination of Br_{org} (Berg and Solomon, 2016). Thus, salt-affected wetlands are not a net source of methyl bromide (Wang *et al.*, 2016; Jiao *et al.*, 2018). However, salt marshes are a net source of methyl bromide (Wang *et al.*, 2016; Jiao *et al.*, 2018), and in the long term, the conversion of salt-affected wetlands into salt marshes with further sea level rise is ultimately likely to release Br_{org} retained in soil to the atmosphere as halomethanes. More work is needed to evaluate the timescale and extent of increased halomethane emissions due to sea level rise.

Our study documents for the first time that a large repository of Br_{org} forms from the reactions of seawater with terrestrial NOM and that the reactions are rapid, on the order of hours to days. Facilitated by changes in water salinity and fluctuating wet/dry seasonal cycles in coastal wetlands, bromination of NOM creates a potentially labile pool of organobromines. Further biotic and abiotic decomposition of NOM may break down these sediment-bound organobromines into either Br^- (Jeong *et al.*, 2011; Krzmarzick *et al.*, 2012) or volatile halomethanes (Huber *et al.*, 2009). The preferential production of organobromines is particularly problematic because Br radicals are an order of magnitude more efficient at destroying stratospheric ozone than Cl radicals (Daniel *et al.*, 1999). As sea levels continue to rise, understanding both the formation

and the breakdown of sediment-bound organohalogens may be crucial for predicting future changes in water quality in salt-affected wetlands and stratospheric ozone.

Acknowledgements

We thank Isaiah Ruhl and staff at the College of Science Major Instrument Cluster (COSMIC) at ODU for NMR analysis and Dr. Pat Hatcher for his assistance in analysing and interpreting NMR data. Thank you also to Aparna Raghu and Chris Habermann for help with the NJ soil study. We also thank the beamline scientists at the Stanford Synchrotron Radiation Lightsource, National Synchrotron Light Source, and Advanced Photon Sources, which all are supported by the Department of Energy, Office of Science, Office of Basic Energy Sciences. Finally, we thank Dr. Anne Morel-Kraepiel for reviewing the manuscript and providing critical comments. This work was funded by the National Science Foundation Geobiology program (award 1529927 to Clemson University and 1529956 to Princeton University) and Princeton University (Princeton Environmental Institute, Fred Fox Class of 1939 Fund, Office of the Dean of the College, and Department of Chemistry). Joe-Wong is supported by the Department of Defense through a National Defense Science and Engineering Graduate Fellowship and a Stanford Graduate Fellowship. Schlesinger is supported by a National Science Foundation Graduate Research Fellowship.

Author Contributions

Joe-Wong and Schlesinger contributed equally to the design and execution of experiments, analysis of the data, and to writing the manuscript and supplementary information. Myneni supervised the project and provided manuscript revisions and feedback. Chow assisted in monitoring of the field site and sample collection and provided input on the manuscript.

Editor: Sophie Opfergelt

Additional Information

Supplementary Information accompanies this letter at <http://www.geochemicalperspectivesletters.org/article1911>.





This work is distributed under the Creative Commons Attribution Non-Commercial No-Derivatives 4.0 License, which permits unrestricted distribution provided the original author and source are credited. The material may not be adapted (remixed, transformed or built upon) or used for commercial purposes without written permission from the author. Additional information is available at <http://www.geochemicalperspectivesletters.org/copyright-and-permissions>.

Cite this letter as: Joe-Wong, C., Schlesinger, D.R., Chow, A.T., Myneni, S.C.B. (2019) Sea level rise produces abundant organobromines in salt-affected coastal wetlands. *Geochem. Persp. Let.* 10, 31–35.

References

- BERG, R.D., SOLOMON, E.A. (2016) Geochemical constraints on the distribution and rates of debromination in the deep seafloor biosphere. *Geochimica et Cosmochimica Acta* 174, 30–41.
- BUTLER, A., WALKER, J.V. (1993) Marine haloperoxidases. *Chemical Reviews* 93, 1937–1944.
- CHOW, A.T., DAI, J., CONNER, W.H., HITCHCOCK, D.R., WANG, J.-J. (2013) Dissolved organic matter and nutrient dynamics of a coastal freshwater forested wetland in Winyah Bay, South Carolina. *Biogeochemistry* 112, 571–587.
- COMBA, P., KERSCHER, M., KRAUSE, T., SCHÖLER, H.F. (2015) Iron-catalysed oxidation and halogenation of organic matter in nature. *Environmental Chemistry* 12, 381–395.
- DANIEL, J.S., SOLOMON, S., PORTMANN, R.W., GARCIA, R.R. (1999) Stratospheric ozone destruction: The importance of bromine relative to chlorine. *Journal of Geophysical Research: Atmospheres* 104, 23871–23880.
- DOYLE, T.W., O'NEIL, C.P., MELDER, M.P.V., FROM, A.S., PALTA, M.M. (2007) Tidal Freshwater Swamps of the Southeastern United States: Effects of Land Use, Hurricanes, Sea-level Rise, and Climate Change. In: Conner, W.H., Doyle, T.W., Krauss, K.W. (Ed.) *Ecology of Tidal Freshwater Forested Wetlands of the Southeastern United States*. Springer, Netherlands, 1–28.
- GOŃI, M.A., THOMAS, K.A. (2000) Sources and transformations of organic matter in surface soils and sediments from a tidal estuary (North Inlet, South Carolina, USA). *Estuaries* 23, 548–564.
- HILTON, T.W., NAJJAR, R.G., ZHONG, L., LI, M. (2008) Is there a signal of sea-level rise in Chesapeake Bay salinity? *Journal of Geophysical Research: Oceans* 113, C09002, doi: 10.1029/2007JC004247.
- HUBER, S.G., KOTTE, K., SCHÖLER, H.F., WILLIAMS, J. (2009) Natural Abiotic Formation of Trihalomethanes in Soil: Results from Laboratory Studies and Field Samples. *Environmental Science & Technology* 43, 4934–4939.
- JEONG, H.Y., ANANTHARAMAN, K., HAN, Y.-S., HAYES, K.F. (2011) Abiotic reductive dechlorination of cis-dichloroethylene by Fe species formed during iron- or sulfate-reduction. *Environmental Science & Technology* 45, 5186–5194.
- JIAO, Y., RUECKER, A., DEVENTER, M.J., CHOW, A.T., RHEW, R.C. (2018) Halocarbon Emissions from a Degraded Forested Wetland in Coastal South Carolina Impacted by Sea Level Rise. *ACS Earth and Space Chemistry* 2, 955–967.
- KRAUSS, K.W., DUBERSTEIN, J.A., DOYLE, T.W., CONNER, W.H., DAY, R.H., INABINETTE, L.W., WHITBECK, J.L. (2009) Site condition, structure, and growth of baldcypress along tidal/non-tidal salinity gradients. *Wetlands* 29, 505–519.
- KRZMARZICK, M.J., CRARY, B.B., HARDING, J.J., OYERINDE, O.O., LERI, A.C., MYNENI, S.C.B., NOVAK, P.J. (2012) Natural Niche for Organohalide-Respiring Chloroflexi. *Applied and Environmental Microbiology* 78, 393–401.
- LERI, A.C., HAY, M.B., LANZIROTTI, A., RAO, W., MYNENI, S.C.B. (2006) Quantitative Determination of Absolute Organohalogen Concentrations in Environmental Samples by X-ray Absorption Spectroscopy. *Analytical Chemistry* 78, 5711–5718.
- LERI, A.C., MYNENI, S.C.B. (2010) Organochlorine turnover in forest ecosystems: The missing link in the terrestrial chlorine cycle. *Global Biogeochemical Cycles* 24.
- LERI, A.C., MYNENI, S.C.B. (2012) Natural organobromine in terrestrial ecosystems. *Geochimica et Cosmochimica Acta* 77, 1–10.
- LERI, A.C., RAVEL, B. (2015) Abiotic Bromination of Soil Organic Matter. *Environmental Science & Technology* 49, 13350–13359.
- LIN, K., SONG, L., ZHOU, S., CHEN, D., GAN, J. (2016) Formation of brominated phenolic contaminants from natural manganese oxides-catalyzed oxidation of phenol in the presence of Br⁻. *Chemosphere* 155, 266–273.
- MOLINA, M.J., ROWLAND, F.S. (1974) Stratospheric sink for chlorofluoromethanes: chlorine atom-catalysed destruction of ozone. *Nature* 249, 810–812.
- MORRISSEY, E.M., GILLESPIE, J.L., MORINA, J.C., FRANKLIN, R.B. (2014) Salinity affects microbial activity and soil organic matter content in tidal wetlands. *Global Change Biology* 20, 1351–1362.
- MUNNS, R., TESTER, M. (2008) Mechanisms of Salinity Tolerance. *Annual Review of Plant Biology* 59, 651–681.
- MYNENI, S.C.B. (2002) Formation of Stable Chlorinated Hydrocarbons in Weathering Plant Material. *Science* 295, 1039–1041.
- NEUBAUER, S.C. (2013) Ecosystem Responses of a Tidal Freshwater Marsh Experiencing Saltwater Intrusion and Altered Hydrology. *Estuaries and Coasts* 36, 491–507.
- RHEW, R.C., MILLER, B.R., WEISS, R.F. (2000) Natural methyl bromide and methyl chloride emissions from coastal salt marshes. *Nature* 403, 292–295.
- TITUS, J.G., RICHMAN, C. (2001) Maps of lands vulnerable to sea level rise: modeled elevations along the US Atlantic and Gulf coasts. *Climate Research* 18, 205–228.
- TUXEN, K., SCHILE, L., STRALBERG, D., SIEGEL, S., PARKER, T., VASEY, M., CALLAWAY, J., KELLY, M. (2011) Mapping changes in tidal wetland vegetation composition and pattern across a salinity gradient using high spatial resolution imagery. *Wetlands Ecology and Management* 19, 141–157.
- WANG, J.-J., JIAO, Y., RHEW, R.C., CHOW, A.T. (2016) Haloform formation in coastal wetlands along a salinity gradient at South Carolina, United States. *Environmental Chemistry* 13, 745.



■ Sea level rise produces abundant organobromines in salt-affected coastal wetlands

C. Joe-Wong, D.R. Schlesinger, A.T. Chow, S.C.B. Myneni

■ Supplementary Information

The Supplementary Information includes:

- Methods
- Sediment Organic Carbon Characteristics
- Laboratory Simulations
- Tables S-1 and S-2
- Figures S-1 to S-9
- Supplementary Information References

Methods

Three sites at Winyah Bay were sampled along a transect from the freshwater wetland to the salt-affected wetland and the salt marsh (Fig. S-1). Soil core samples were collected using an AMS multi-stage soil core sampler. In brief, a stainless-steel cylinder (5 cm diameter, 30 cm length) with a plastic liner was vertically inserted into the soil. 24 cm soil cores from the freshwater wetland were collected between July 2012 and December 2016, and 18-24 cm soil cores from the salt-affected wetland and salt marsh were collected during low tide and high tide in summer 2012. All cores were immediately sealed on both ends with plastic caps and placed in ice coolers. The cores were then shipped to Princeton University, where they were horizontally divided into 3-4 cm sections and stored at 4 °C. Total Br and Cl concentrations and speciation in the salt-affected wetland and salt marsh were determined to be relatively consistent with depth and at low and high tide due to consistent salt water inundation, so these sites were not tested over multiple seasons. In the freshwater wetland, however, temporal differences in total halogen concentration were expected and observed in the freshwater wetland, and thus samples were taken over multiple seasons. To determine the seasonal variability in Br concentrations, multiple freshwater wetland cores were collected during both wet and dry seasons (2012-2016).

Water salinity at each site was measured monthly using a portable YSI salinity meter. In the freshwater and salt-affected wetlands, piezometers have been installed approximately 50 cm below soil surfaces since 2005, and these were used for salinity measurements. A minimum of 1 L of water was manually pumped out from the piezometers before measuring salinity. In the salt marsh, the YSI probe was gently placed approximately 10-20 cm below water surface to measure salinity.

The quality of the sedimentary organic carbon in freshwater, salt-affected wetland, and salt marsh samples was analysed using Fourier Transform Infrared (FTIR) spectroscopy and solid-state ¹³C Nuclear Magnetic Resonance spectroscopy (NMR). The FTIR spectra were obtained using a diamond attenuated total reflectance-FTIR (ATR-FTIR) on a Bruker IFS 66 V/S using a DTGS detector. Samples were freeze-dried, and 100 scans were collected per sample with a 2.0 cm⁻¹ resolution and an aperture setting of 6 mm. The ATR crystal surface was cleaned with water and dried between each sample run. Samples were prepared for NMR analysis by freeze-drying. NMR spectra were collected at the COSMIC facility at Old Dominion University on a 400 MHz AVANCE II NMR equipped with a 4 mm solid-state CPMAS probe. The samples were spun at 14000 Hz, and the spectra were calibrated externally to glycine. A CP-multipulse experiment was used to obtain each spectrum, and the delay times were optimised for plant-like and soil materials. Spectra from FTIR and NMR were analysed using GRAMS/AI Spectroscopy Software.

Sediment samples from freshwater wetlands in Winyah Bay were reacted with Br⁻ concentrations ranging from 0.1x to the concentration of seawater (0.1-1.0 mM Br⁻). Sample set 1 was reacted solely with Br⁻ by adding an aqueous KBr solution. Sample set 2 was prepared at the same Br⁻ concentrations with additional Cl⁻ as aqueous KCl at relative sea water concentrations (*i.e.* 680 times the concentration of Br⁻ in each sample) (Ensign *et al.*, 2013). Sample set 3 was prepared with Br⁻, Cl⁻, and with solution pH maintained at 8.1, the approximate pH of seawater (Ensign *et al.*, 2013). pH of the solution before addition to soil was measured using a pH probe and was adjusted by the addition of NaHCO₃ until the desired pH was reached.

For all sample sets, experiments were conducted in saturated and wet/drying cycle conditions intended to mimic the differences between salt marsh and salt-affected wetland, respectively. In saturated samples, 2 g of soil was placed in 3 mL of solution, and samples were closed to the atmosphere (head space ~45 mL). In the wet-dry experiments, 2 grams of soil was exposed to a total of 3.0 mL of solution over the course of one month, with approximately 2-3 drops added every other day. These samples were partially open to the atmosphere, allowing them to dry in between wetting periods. For both saturated and wet-dry experiments, reactions were initiated on the same day and both sample sets were analysed after one month of reaction time. The reacted samples were analysed using X-ray spectroscopy for halogen speciation and concentrations.

For all samples, the total concentrations of Cl and Br were estimated using X-ray fluorescence spectroscopy, and their speciation was determined using synchrotron-based X-ray absorption near-edge structure spectroscopy (XANES) (Figs. 1, S-2, Table S-1).

For XRF analysis of natural samples, samples were air-dried and ground for 20 minutes in a micronising mill before homogenisation with a cellulose binder (5 wt. %). Poly(acrylic acid) (molecular weight 2100 amu) was added if less than 5 g of sample was available. Laboratory-incubated samples were dried in an oven at 50 °C overnight and ground using a diamond mortar and pestle. These samples were mixed with a cellulose binder for a total mass of 7 g. All samples were pressed into a disposal aluminum cup in a 40 mm die under at least 4 tons of pressure for 2 minutes using a standard laboratory hydraulic press. Pellets were stored in a desiccator and heated at 65 °C for at least one hour immediately prior to analysis to drive off remaining water. XRF analysis was conducted using a Rigaku Supermini200 X-ray fluorescence spectrometer. An RX25 crystal and scintillation counter were used to detect Cl, and a LiF crystal and gas flow proportional counter were used to detect Br. All sample pellets were analysed in a vacuum environment. A built-in semi-quantitative analysis program and a set of Br and Cl standards was used to determine elemental concentrations.



Cl 1s XANES spectra were collected at the National Synchrotron Light Source (NSLS) at Brookhaven National Laboratory (Upton, New York) on beamlines X15B and X19A and at the Stanford Synchrotron Radiation Light Source (SSRL) (Menlo Park, CA) on beamline 4-3. For X15B, partially air-dried samples were mounted in X-ray-clean, halogen-free polypropylene film envelopes in a He-purged sample chamber. The beamline was equipped with higher-order rejection mirrors, and the beam was fully tuned during data collection. A Ge detector measured sample fluorescence signal in 0.1 eV increments of the incident photon energy around the Cl absorption edge. For X19A, partially air-dried samples were mounted on polypropylene holders between halogen-free Kapton tape and polypropylene film. The side covered with propylene film was exposed to the beam in a He-purged sample chamber. The monochromator was detuned by 50 % to screen out harmonics. For 4-3, samples were mounted between X-ray-clean, halogen-free polypropylene film and analyzed in a He sample chamber. The beamline utilised a collimated and unfocused beam to allow for bulk sample analysis. A Canberra PIPS detector (X19A) or vortex detector (4-3) was used to measure sample fluorescence, and XANES spectra were collected around the Cl 1s absorption edge. A chlorophenol red standard was measured periodically, and scans were calibrated with the Cl 1s absorption maximum of chlorophenol red at 2821.1-2821.2 eV (Leri *et al.*, 2006).

Scans were calibrated and averaged using Demeter (version 1.9.09) (Ravel and Newville, 2005). The spectra were normalised in Demeter by fitting a first-order polynomial to the pre-edge region and a first- or second-order polynomial to the post-edge region. Cl speciation was determined by linear least squares fitting to a library of Cl standards with less than 6 % uncertainty (Leri *et al.*, 2006). Selected spectra were reprocessed in WinXAS (version 2.0) to verify the results from Demeter (Ressler, 1998).

Br 1s XANES spectra were collected at NSLS on beamline X19A, at SSRL on beamline 4-1, and at the Advanced Photon Source (APS) at Argonne National Laboratory (Lemont, Illinois) on beamline 13-IDE. Samples were prepared and mounted as for Cl XANES spectroscopy. A 13-element Ge detector (NSLS, SSRL) or vortex ME4 silicon drift diode array detector (APS) measured sample fluorescence around the Br 1s absorption edge. A 4-bromophenol or KBr (aq) standard was taken continuously, and scans were calibrated with the Br 1s pre-edge local absorption maximum of 4-bromophenol at 13473.6 eV or Br 1s absorption maximum of KBr at 13477.3 eV (Leri *et al.*, 2010). Spectra were processed in Demeter and WinXAS as described above.

Cl and Br bound to aliphatic organic carbon give rise to slightly lower-energy edges than Cl and Br bound to aromatic organic carbon, respectively (Fig. 1). By comparing with the spectra of model Cl and Br compounds, the fractions of aliphatic, aromatic, and inorganic Cl and Br can be estimated in unknown natural samples without subjecting sediments to destructive analysis. The absolute concentrations of these different pools of Cl and Br were determined by combining this speciation data from XANES spectroscopy with total halogen concentrations derived from XRF.

Sediment Organic Carbon Characteristics

The organic carbon concentrations, nitrogen concentrations, and C/N ratios at each site are shown in Table S-2. The N concentration and C/N ratio are generally used as an indicator of the extent of plant material biodegradation in soil systems. They have been included here as a reference for microbial activity, though the C/N ratio is consistent between soil depths and thus does not appear to have an effect on the halogenation reactions in this study. The quality of organic carbon was assessed with FTIR and NMR. In the FTIR spectra shown in Figure S-5, for both the freshwater wetland and salt marsh, representative peak intensities for aliphatic/carbohydrate organic carbon (950-1150 cm^{-1}) are larger than those in the aromatic/carbonyl region (around 1630 cm^{-1}), whereas the opposite trend is observed in the salt-affected wetland. Although FTIR peak areas do not represent absolute concentrations of aromatic or aliphatic carbon, they qualitatively indicate that the salt-affected wetland samples are richer in aromatic/carbonyl type organic matter relative to the two other locations. The NMR spectra provide a quantitative view of the organic carbon functional groups and helps to confirm trends observed in the total carbon analysis and in the FTIR analysis. The NMR spectrum for the salt-affected wetland has a greater intensity across the entire spectrum compared to the other two sites (Fig. S-6a). This is consistent with the greater than threefold increase in total organic carbon in the salt affected wetland (Table S-2). Moving across the salinity gradient from the freshwater wetland to salt marsh, the NMR peak area for aromatic carbon (100-160 ppm) is highest in the salt-affected wetland. The peak area for aliphatic content (5-50 ppm) increases across the gradient with increasing salinity (Fig. S-6a).

Spectral contributions of aromatic and aliphatic carbon were determined by integrating the peak area of each region in both FTIR and NMR spectra for each site. FTIR and NMR spectra cannot be directly compared because the region in which aromatic features are observed in the IR spectra overlaps with the regions where protein and carboxyl features are observed. Thus, the aromatic peak area determined from the IR spectra is likely artificially inflated by the presence of protein and carboxyl groups. Nevertheless, both techniques show that the ratio of aromatic peak area to aliphatic peak area changes significantly between sites (Fig. S-7). The salt marsh shows significantly higher levels of aliphatic carbon compared to the salt-affected wetland and thus has a very low aromatic:aliphatic ratio. This salt marsh primarily contains cordgrass and rush grass, which largely consist of cellulose and waxy hydrocarbon type organic material and contribute aliphatic carbon to NOM. In particular, the two sharp peaks in the



aliphatic regions at 30 and 33 ppm represent two types of long-chain polymers associated with waxy cuticles of plant matter (Müssig, 2010). These groups are much more abundant in the salt-affected and salt marsh samples when compared to the freshwater wetland, most likely due to vegetation changes that occur as a result of seawater intrusion. The salt-affected wetland, which has a very high aromatic:aliphatic ratio, contains not only a mix of grasses but also deceased trees such as bald cypress that are common to freshwater wetlands. These decaying trees are a source of lignin and related aromatic compounds (Müssig, 2010). Aromatic-type organic matter is more prone to electrophilic addition by Br species and combined with the overall total increase in organic carbon content (Table S-2), this is likely a major contributing factor to the observed increase in organobromine production in the salt-affected wetland compared to the freshwater wetland or salt marsh.

The freshwater wetland was sampled at three different times of the year to assess different seasonal and climatic conditions that may affect the carbon content in the wetlands. NMR analysis of these samples showed similar patterns and intensities indicating no significant changes in aromatic and aliphatic carbon content between the seasons (Fig. S-6b).

Laboratory Simulations

Samples prepared with both Br⁻ and Cl⁻ (unregulated pH, sample set 2) and with Br⁻, Cl⁻, and kept at pH 8.1 (sample set 3) showed no systematic changes in organobromine production when compared with samples that were reacted only with Br⁻ (Fig. S-8). Variability observed in these samples is small enough to likely be a result of sample heterogeneity. The saturated samples in sample set 3 show consistently lower percentage organobromine, which may be a result of competing reactions with NaHCO₃. Wet/dry samples, however, show consistent organobromine production in all conditions, indicating that chlorination of NOM does not significantly compete with bromination in salt-affected wetlands.

Laboratory simulations of bromination reactions were also tested on pristine, freshwater wetland soil collected from a temperate, pine forest, the Pine Barrens, New Jersey. Results from adding Br⁻ to a New Jersey soil core show that all of the added Br was converted to organobromine (Fig. S-9). The Pine Barrens ecosystem differs from the Winyah Bay significantly in vegetation type, leading to a different soil organic carbon profile. The Winyah Bay freshwater wetland site is forested and dominated in vegetation by bald cypress (*Taxodium disticum*), water tupelo (*Nyssa aquatic*), and swamp tupelo (*Nyssa sylvatica* var. *biflora*). The Pine Barrens site's vegetation is dominated mainly by various types of maple, oak, and pine trees. The ubiquity of bromination reactions in both these conditions suggests that bromination is potentially favorable in a broad range of soil ecosystems.



Supplementary Tables

Table S-1 Abundance and speciation of Cl and Br in sediments; Cl⁻ partitioning coefficient; and Cl and Br relative retention in sediments from Winyah Bay, South Carolina. Every datum is the average of two cores, which showed minimal differences. $K_d(\text{Cl}^-)$ is identical to $K_d(\text{Cl}_{\text{total}})$ for the salt-affected wetland and salt marsh due to the low fraction of Cl_{org} at these sites (as determined with XANES spectroscopy). ND: Not determined because low abundance of Cl resulted in poor-quality Cl XANES spectra that could not be fit to determine the speciation of Cl.

Location	Depth (cm)	Maximum surface salinity (ppt)	Cl _{total} (g/kg)	Cl _{org} (g/kg)	Cl _{org} / Cl _{total}	Br _{total} (mg/kg)	Br _{org} (mg/kg)	Br _{org} / Br _{total}	K _d (Cl)	$\frac{(\text{Br}/\text{Cl})_{\text{sediment}}}{(\text{Br}/\text{Cl})_{\text{water}}}$
Freshwater wetland	2	0.34	0.27	0.16	0.62	24	21	0.87	0.5	26.5
	6		0.17	ND	ND	15	13	0.90	0.3	24.9
	10		0.16	0.11	0.73	10	7	0.74	0.2	18.9
	14		0.092	ND	ND	7	6	0.99	0.1	23.3
	18		0.091	ND	ND	4	3	0.77	0.1	11.9
	22		0.069	ND	ND	2	1	0.97	0.1	7.4
Salt-affected wetland	2	10.09	5.64	0.21	0.05	173	152	0.87	1.0	8.9
	6		7.93	0	0.00	154	145	0.95	1.4	5.7
	10		6.61	0.08	0.01	101	97	0.94	1.2	4.2
	14		6.47	0.24	0.04	95	92	0.94	1.2	4.2
	17		6.92	0	0.00	135	123	0.87	1.3	5.7
	22		4.52	0.79	0.17	69	69	1.00	0.8	4.4
Salt marsh	2	27.43	27.48	0	0.00	160	88	0.58	1.8	1.7
	5		26.76	0	0.00	181	99	0.55	1.8	2.0
	8		24.09	1.06	0.04	138	62	0.45	1.6	1.7
	11		26.90	0	0.00	165	75	0.46	1.8	1.8
	14		30.15	0	0.00	155	82	0.53	2.0	1.5
	18		30.07	0	0.00	165	79	0.47	2.0	1.6



Table S-2 Sedimentary organic carbon and nitrogen along the salinity gradient.

Location	Depth (cm)	% weight		Molar ratio
		N	C	C/N
Freshwater wetland	0-10	0.46	7.26	15.75
	10-20	0.50	8.54	17.21
	20-30	0.39	6.27	15.93
Salt-affected wetland	0-10	1.36	29.03	21.40
	10-20	1.51	25.36	16.80
	20-30	1.57	30.80	19.61
Salt marsh	0-10	0.41	8.84	21.33
	10-20	0.19	3.38	17.56
	20-30	0.37	8.27	22.31



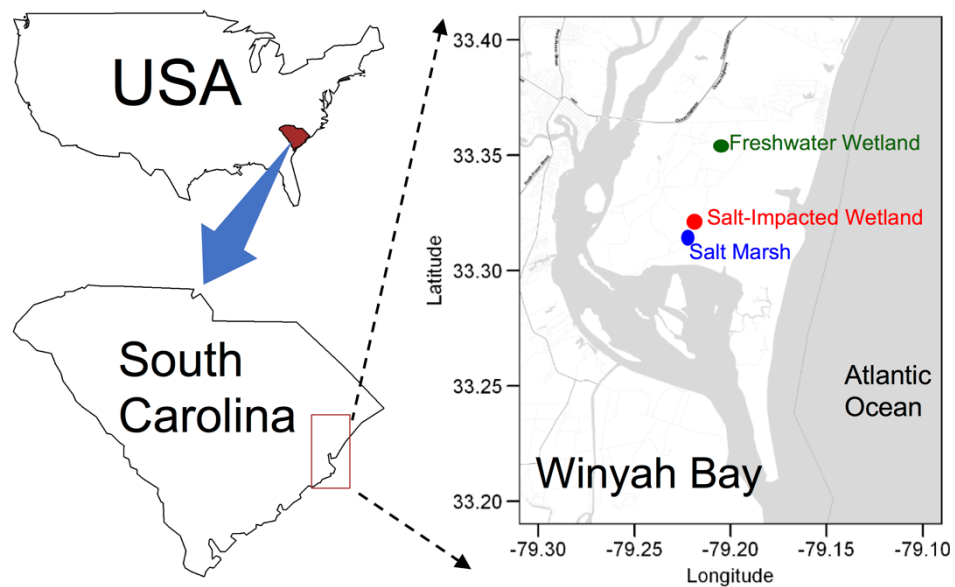
Supplementary Figures

Figure S-1 Map of the sampling site at Winyah Bay, South Carolina, United States.

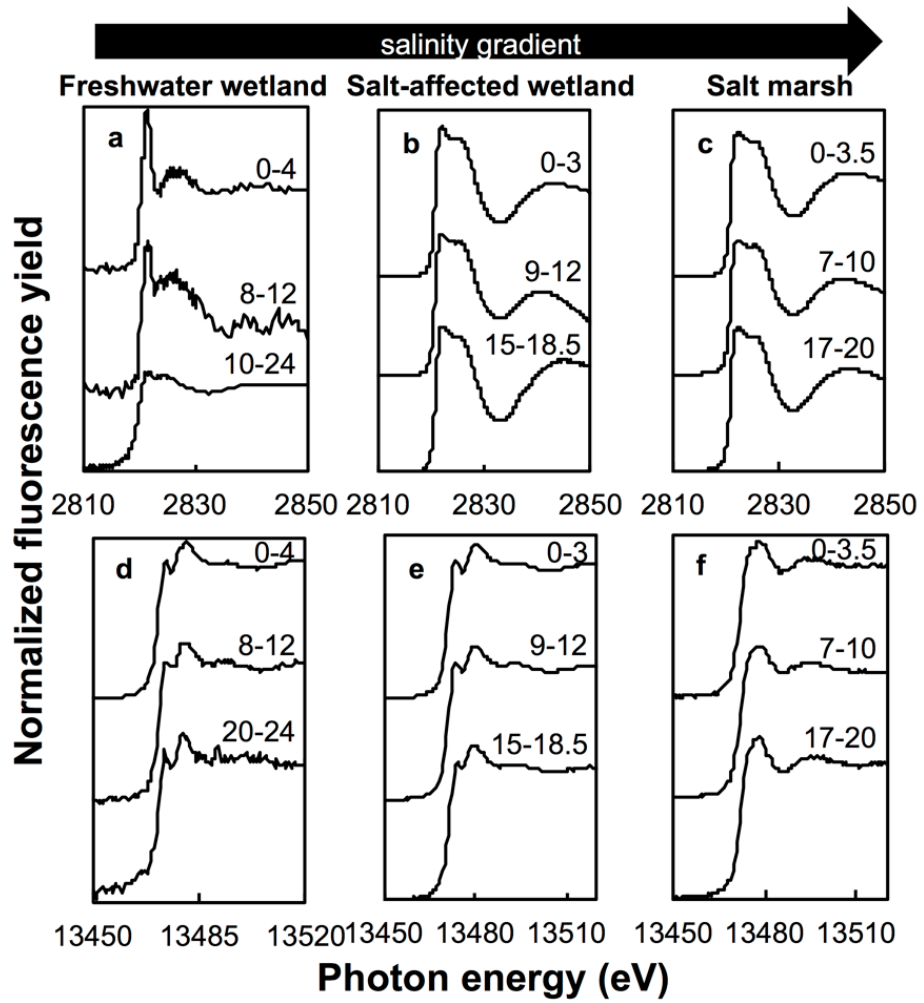


Figure S-2 Normalised Cl (top, a-c) and Br (bottom, d-f) K-edge XANES spectra of sediments from Winyah Bay, South Carolina at representative top, middle, and bottom depths, as indicated in cm.

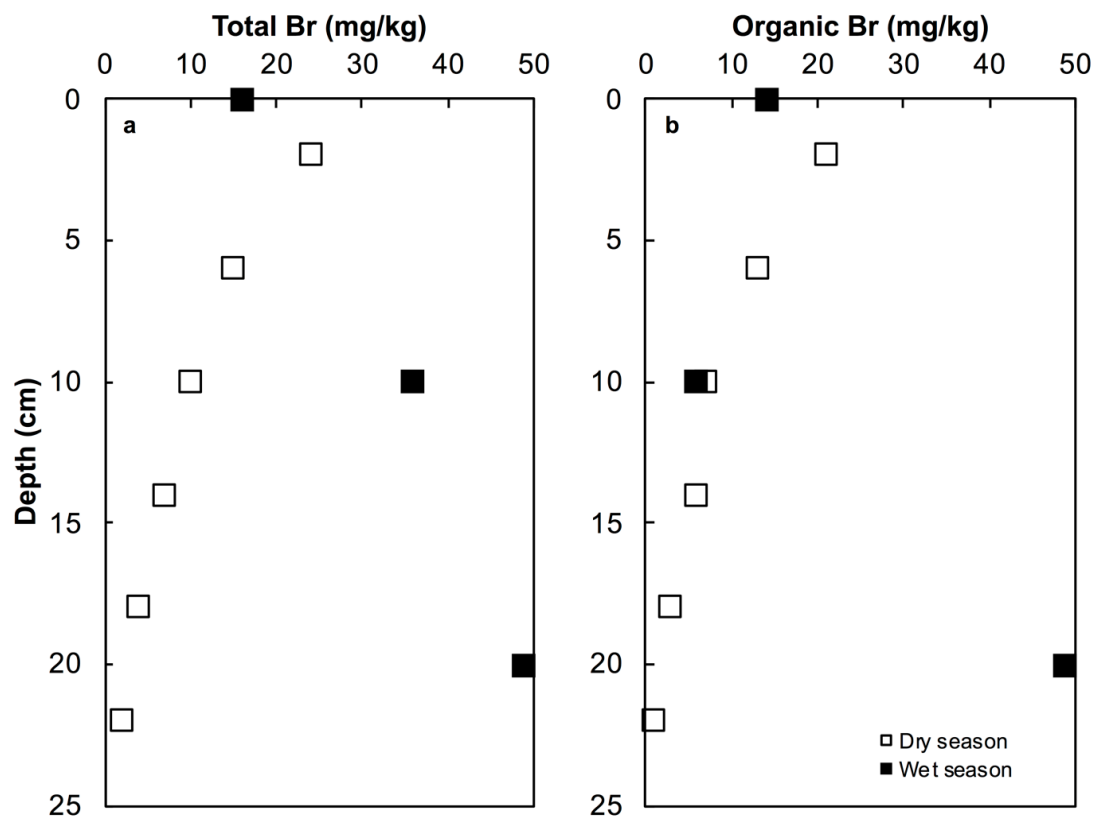


Figure S-3 Seasonal fluctuations in bromine concentrations in the freshwater wetland. (a) Total Br concentrations (mg/kg) and (b) organobromine concentrations (mg/kg) measured as a function of depth in freshwater wetland samples collected in two different seasons.

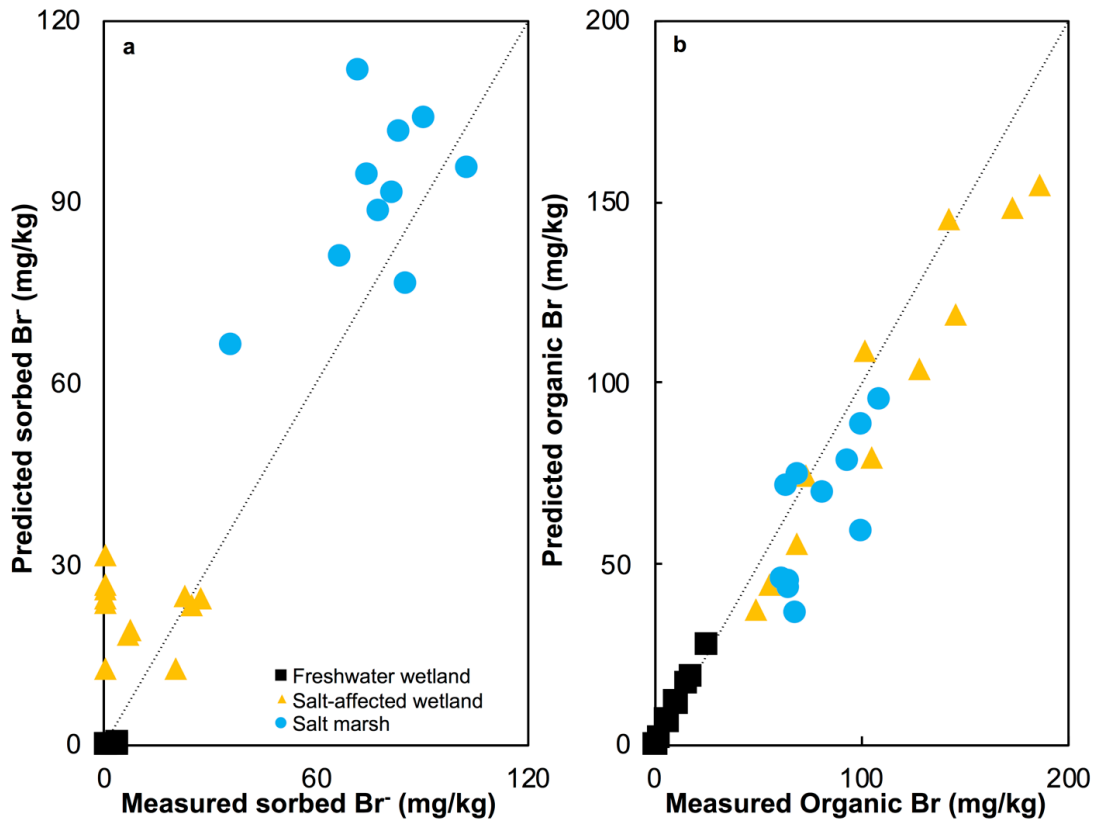


Figure S-4 Correlations of predicted and measured (a) sorbed Br⁻ and (b) organobromine concentrations in sediments. Predicted sorbed Br⁻ and organobromine for each site were derived using $K_d(\text{Cl}^-)$. This is because Cl⁻ and Br⁻ are inert and considered to exhibit similar adsorption onto soil and sediment particles (predicted sorbed Br⁻ = $\text{Br}^-_{\text{water}} \cdot K_d(\text{Cl}^-)$). Predicted Br_{org} = measured Br_{total} - predicted sorbed Br⁻.

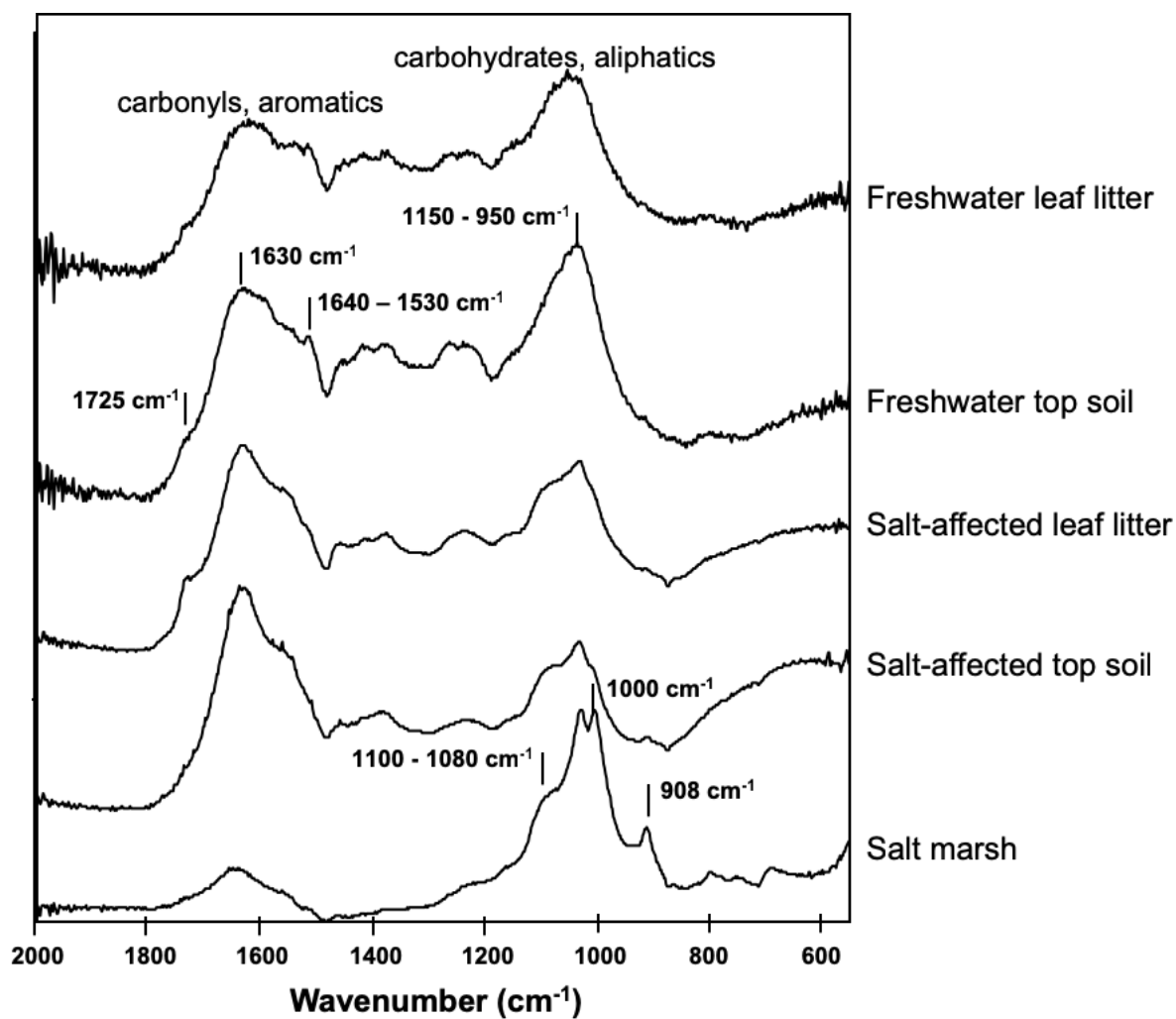


Figure S-5 FTIR spectra of wetland sediments along the salinity gradient. The representative FTIR peaks of humic substances, as labeled in the figure, are: 1725 cm^{-1} – C=O stretch of carboxylic acid; 1630 cm^{-1} – broad peak of both nitration and C=C aromatic stretch; $1640-1530 \text{ cm}^{-1}$ – NH_2 in plane bend, and C=O of amide bond; $1150 - 950 \text{ cm}^{-1}$ – C-OH (alcohol), C-C, and C-H broad absorption bands and C-N stretch of amine at 1030 cm^{-1} ; $1100-1080 \text{ cm}^{-1}$ – aqueous inorganic and organo-sulfate; 1000 cm^{-1} – Si-O stretch; 908 cm^{-1} – inorganic sulfate symmetric stretch.

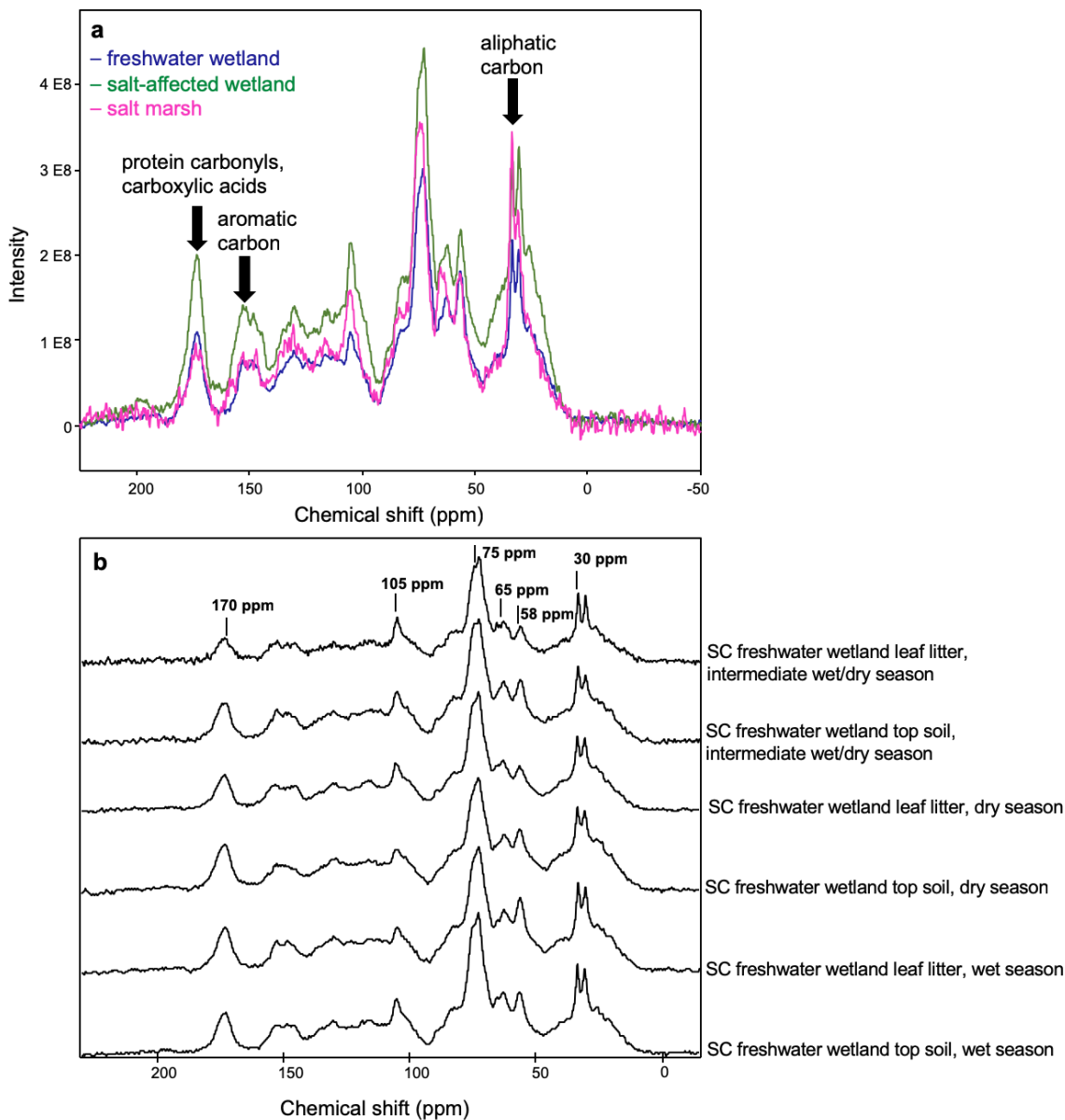


Figure S-6 (a) NMR spectra collected for each of the wetland conditions across the salinity gradient. (b) NMR spectra collected for freshwater wetland leaf litter and top soil over multiple seasons. The representative peaks of humic substances are: 5-50 ppm – aliphatic region; 30 ppm, 33 ppm – strong aliphatic region peak for humic acids and long chain polymers; 50-100 ppm - chemical shift region of carbohydrates and carbons singly substituted with electronegative substituents; 58 ppm - most likely that of -OCH₃ carbon, terrestrial humic acids; 65 ppm - 6 carbon in hexose monomers; 75 ppm - 2, 3, 4, and 5 carbons in hexose monomers; 105 ppm - anomeric carbons of polysaccharides; 100-160 ppm – aromatic carbon resonances; 170 ppm – protein carbonyls and carboxylic acids.



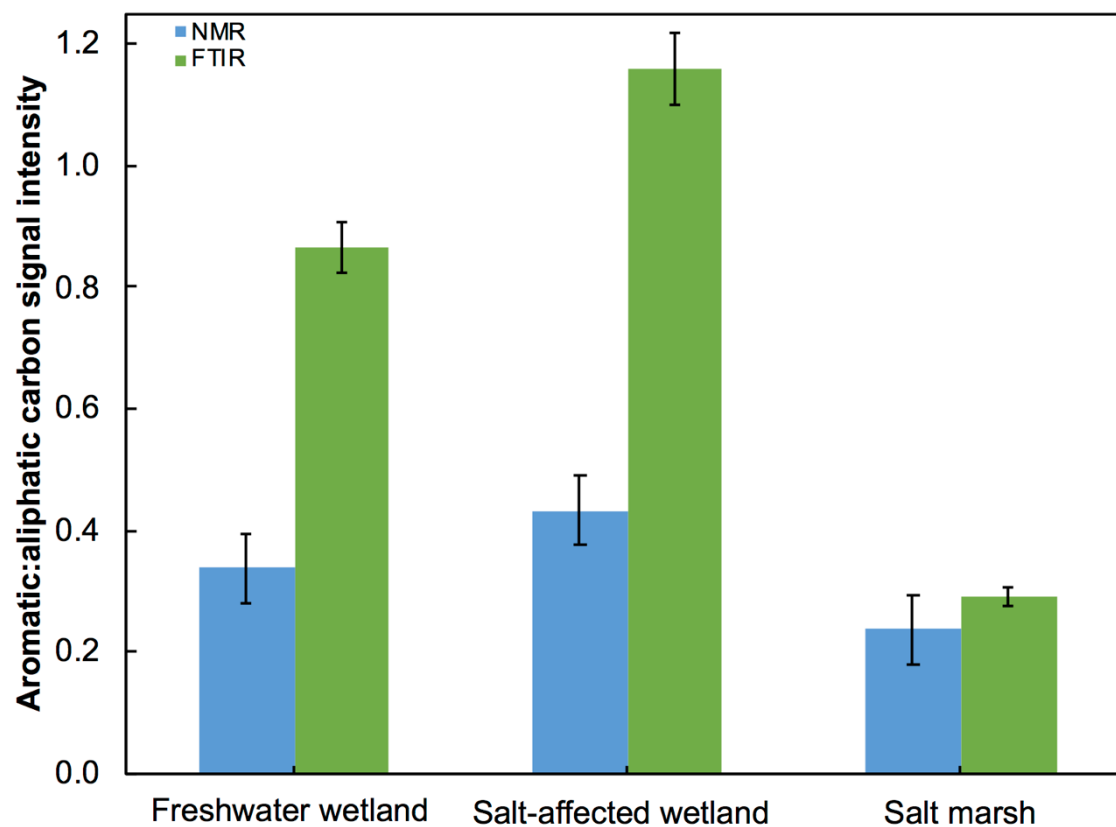


Figure S-7 Ratio of aromatic to aliphatic carbon composition in different wetland sites from FTIR and NMR analysis.

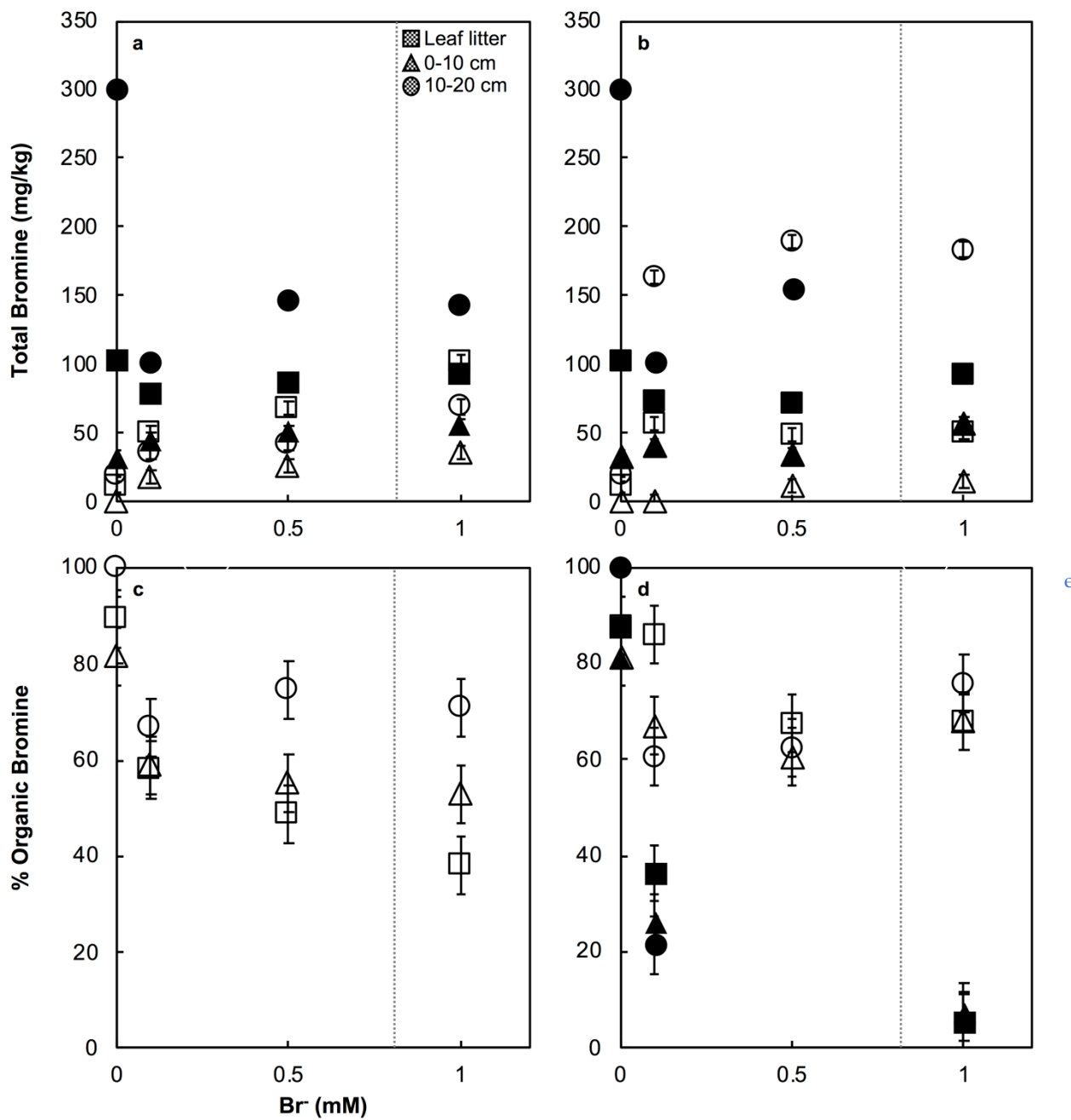


Figure S-8 Total Br retention (top) and percent organobromine production (bottom) in freshwater sediments: **(a)** total Br in samples reacted with Br^- and Cl^- , **(b)** total Br in samples reacted with Br^- and Cl^- at elevated pH 8.1, **(c)** percent organobromine in samples reacted with Br^- and Cl^- , and **(d)** percent organobromine in samples reacted with Br^- and Cl^- at elevated pH 8.1. These figures incorporate the wet season percent organobromine for the data point at 0-10 cm and 0.0 mM Br^- , although we found that the samples are heterogeneous and change with location and seasons. Some error bars are smaller than the symbols.



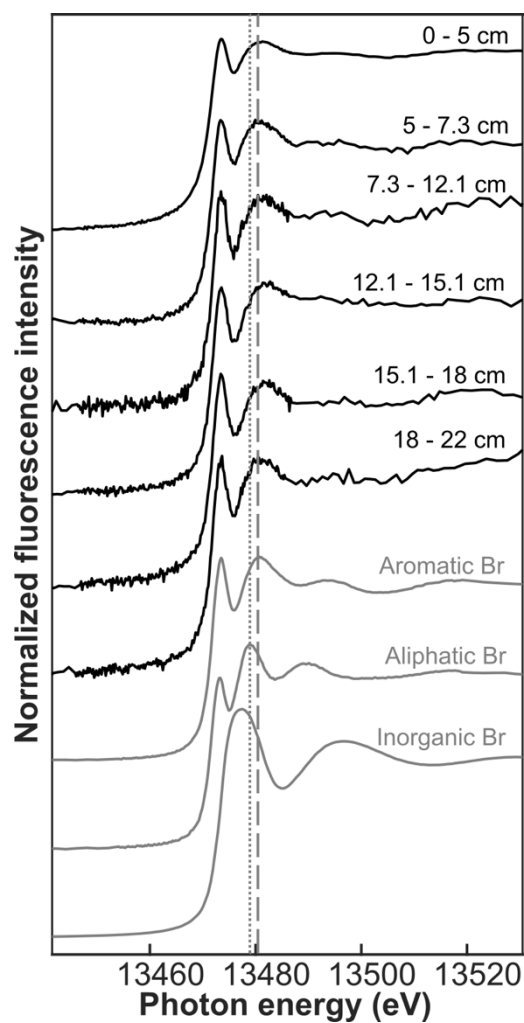


Figure S-9 Speciation of Br in Pine Barrens, New Jersey freshwater wetland soil reacted with aqueous Br⁻. The Br XANES spectra show that all added Br⁻ is converted to Br_{org} within 60 days under air-dried conditions. As in Figure 1, Br standards are bromophenol blue, 1-bromoeicosane, and KBr for aromatic, aliphatic, and inorganic Br respectively. Spectral maxima for aliphatic and aromatic organohalogen standards are shown in grey dotted and dashed lines respectively.

Supplementary Information References

- Ensign, S.H., Hupp, C.R., Noe, G.B., Krauss, K.W., Stagg, C.L. (2013) Sediment Accretion in Tidal Freshwater Forests and Oligohaline Marshes of the Waccamaw and Savannah Rivers, USA. *Estuaries and Coasts* 1–13.
- Leri, A.C., Hakala, J.A., Marcus, M.A., Lanzirotti, A., Reddy, C.M., Myneni, S.C.B. (2010) Natural organobromine in marine sediments: New evidence of biogeochemical Br cycling. *Global Biogeochemical Cycles* 24, doi: 10.1029/2010GB003794.
- Leri, A.C., Hay, M.B., Lanzirotti, A., Rao, W., Myneni, S.C.B. (2006) Quantitative Determination of Absolute Organohalogen Concentrations in Environmental Samples by X-ray Absorption Spectroscopy. *Analytical Chemistry* 78, 5711–5718.
- Müssig, J. (2010) *Industrial Applications of Natural Fibres: Structure, Properties and Technical Applications*. John Wiley & Sons, Chichester, UK.
- Ravel, B., Newville, M. (2005) Athena, Artemis, Hephaestus: data analysis for X-ray absorption spectroscopy using IFEFFIT. *Journal of Synchrotron Radiation* 12, 537–541.
- Ressler, T. (1998) WinXAS: a program for X-ray absorption spectroscopy data analysis under MS-Windows. *Journal of Synchrotron Radiation* 5, 118–122.

